Monitoring PMD-Induced Penalty and Other System Performance Metrics via a High-Speed Spectral Polarimeter

Shawn X. Wang, *Student Member, IEEE*, Andrew M. Weiner, *Fellow, IEEE*, Misha Boroditsky, *Senior Member, IEEE*, and Misha Brodsky, *Member, IEEE*

***Abstract*—We developed and tested a nonintrusive technique for estimating polarization-mode-dispersion-induced system penalties based on spectral polarization measurements. Other system characteristics such as power fluctuations and carrier-frequency drift could also be monitored simultaneously. Our spectral polarimeter works in milliseconds, and can be scaled to monitor all channels in the C-band.**

***Index Terms*—Optical fiber communications, polarimetry, polarization-mode dispersion (PMD), system performance.**

I. Introduction

THE ABILITY to evaluate the impact of polarization-mode dispersion (PMD) on optical communications systems separately from other impairments is important for PMD monitoring, mitigation, and compensation schemes. Many common types of signals used for PMD-penalty estimation such as degree of polarization (DOP), radio-frequency (RF) spectrum, and the eye opening have been reviewed [1]. DOP has been shown to be sensitive to noise loading, while the latter methods require expensive equipment such as RF spectrum analyzers and gigahertz oscilloscopes; and all these methods monitor one channel at a time. Recently, the state of polarization (SOP) "string" length [2] has been demonstrated to have strong correlation with PMD-induced penalty in a channel. The SOP string represents the length of the wavelength-dependent SOP trace on the Poincarè sphere over the modulation bandwidth of the channel. In [2], the differential group delay (DGD) τ and the angle θ between the PSP and the launch SOP were first measured directly, and then the string length was estimated using a first-order approximation $L_1 = (\tau/T)\sin\theta$. While such an extensive approach is suitable for laboratory studies, these DGD and PSP measurements are less appropriate for live system applications, for which the required switching of the launch SOP among two or more significantly different states (e.g., Mueller matrix method) departs from accepted practice. The previously reported method for measuring high resolution SOP string using heterodyne polarimetry [3] is time consuming, requires the use of expensive test equipment, and is more suited for the laboratory experiments. In this letter, we demonstrate nonintrusive, near real-time estimation of PMD-induced system penalty from direct measurements of the output SOP string lengths using a custom built high-speed high spectral-resolution polarimeter [4]. The spectrometer property of the polarimeter also allows us to monitor other system characteristics such as power fluctuations and carrier-frequency drift of the channels. Following the laboratory experiments, the polarimeter was used in a field trial, monitoring a route carrying live traffic between two major U.S. cities.

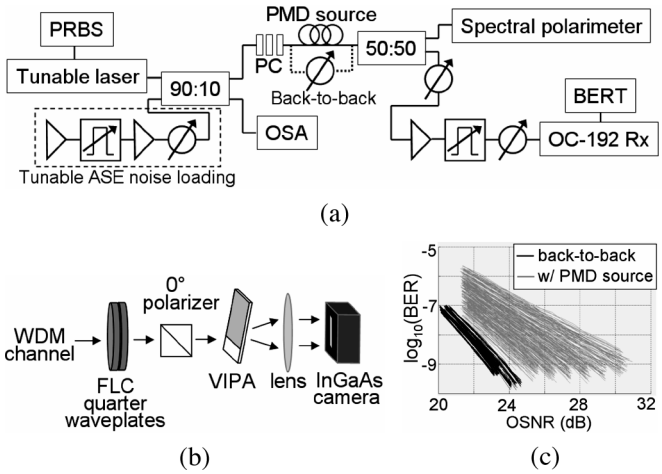

Fig. 1. (a) Experimental setup for measuring OSNR, BER, and SOP string length. (b) Schematic of the high resolution spectral polarimeter. (c) Dependence of BER on OSNR for multiple channels and various launch SOP conditions.

II. Experimental Setup and Results

In the laboratory experimental setup shown in Fig. 1(a), an optical signal was generated by a tunable laser source with an integrated modulator which transmitted a $2^{23}-1$ nonreturn-to-zero (NRZ) pseudorandom binary sequence at 10 Gb/s. Optical signal-to-noise ratio (OSNR) was controlled by loading the signal with amplified spontaneous emission. Ten percent of the signal at the output of the coupler was used for OSNR measurement using an optical spectrum analyzer, and 90% was sent via a polarization controller into a PMD source. Two different mechanically and thermally stabilized PMD sources were tested separately to characterize the relationship between PMD and system performance. One was a polarization-maintaining

Manuscript received January 27, 2006; revised June 2, 2006. This work was supported in part by the National Science Foundation under Grant 0501366-ECS.

S. X. Wang and A. M. Weiner are with the School of Electrical and Computer Engineering, Purdue University, West Lafayette, IN 47907-1285 USA (e-mail: wang7@ecn.purdue.edu; amw@ecn.purdue.edu).

M. Boroditsky and M. Brodsky are with AT&T Laboratories, Middletown, NJ 07748 USA (e-mail: Boroditsky@research.att.com; Brodsky@research.att.com).

Digital Object Identifier 10.1109/LPT.2006.880779

(PM) fiber with 40-ps DGD; the second was a 12-km high-PMD fiber with a mean DGD of 30.8 ps. At the output of the PMD source, the signal was split between a bit-error-rate tester and a high-speed high spectral-resolution polarimeter [4]. The polarimeter had two main parts [see Fig. 1(b)]. The first was a fast polarization analyzer comprised of a pair of ferroelectric liquid crystal switchable quarter-waveplates and a fixed polarizer. The second part utilized a virtually imaged phased array (VIPA, donated by Avanex Corp.) [5] and an InGaAs line-scan camera which allowed one full set of spectrally resolved SOP measurements within 20 ms (software limited), this is the fastest spectral polarimeter reported to our knowledge. In an independent experiment, we have verified 1-ms SOP measurement time for 256 spectral components by employing external timing circuits into the setup. The VIPA was used for its extremely large angular dispersion to achieve required 3-dB resolution of $\sim$1 GHz [6]. The high resolution is necessary to resolve the SOP variations within a 10-Gb/s dense wavelength-division-multiplexing channel bandwidth. Other spectral polarimeter designs [7], [8] lack substantially either in speed and/or spectral resolution.

The camera's pixel spacing corresponds to approximately 1 GHz; 11 pixels were taken to cover 10 GHz ($\Delta\omega = 2\pi \times 10^{10}$ rad/sec) of the 10-Gb/s NRZ modulation bandwidth. The SOP string measured at the output of the PM fiber ($\tau = 40$ ps) covered a maximum distance of 2.5 rad ($\Delta\theta = \tau\Delta\omega$) on the surface of the Poincarè sphere, equivalent to 0.25 rad of SOP difference between neighboring pixels. Although for this first demonstration only one channel was tested at a time using the VIPA-camera pair, the setup can be modified with a two-dimensional (2-D) spectral dispersion arrangement [9] to measure all channels in the entire C-band in parallel.

For the all-order PMD source and the back-to-back measurements, signals were generated at 21 channels with 50–GHz spacing from 193.00 to 194.00 THz on the ITU grid, and 20 different SOP states were launched for each channel. Data were taken for OSNR, BER, and spectral SOP for each channel and at each launch polarization state. To characterize the relationship between PMD and system performance, we measured the change in OSNR penalty relative to the back-to-back measurements [Fig. 1(c)], at a constant bit-error-rate (BER) of 10^{-9}. The same procedure was used for the pure first-order PMD measurement by replacing the all-order PMD fiber with the PM fiber; measurements were then taken from eight 100-GHz-spaced channels from 193.00 to 193.70 THz on the ITU grid.

For each launch polarization condition, the measured output SOP was plotted on the Poincarè sphere, and the distances between neighboring SOP points were summed for 11 consecutive points, centered at the carrier frequency. The total distance was taken as the SOP string length L, measured in radians. It has been shown that the PMD-induced OSNR penalty ε has a quartic relation with the first-order PMD string length $\varepsilon = AL_1^2/4 + BL_1^4$ [2]. The string length for each launch SOP was plotted against its respective OSNR penalty measured at BER $= 10^{-9}$, and then fit to a quartic curve for the pure first-order PMD data (see Fig. 2) netting the coefficients $A = 3.76$ and $B = 0.12$. A constant term of 0.35 was also observed due to penalty spread, thus the nonzero penalty curve at 0 rad string length. Since the pure first-order string length is known

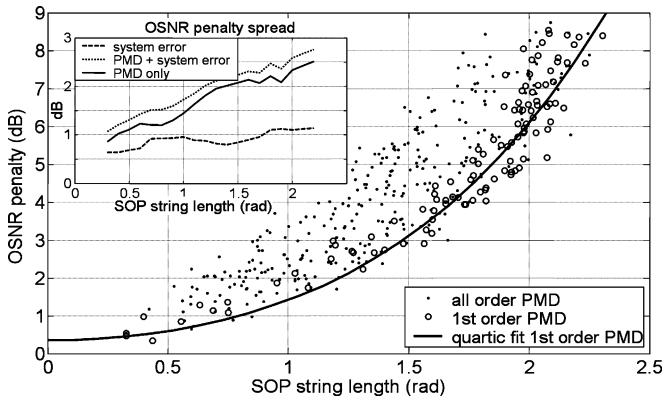

Fig. 2. SOP "string" length versus PMD-induced OSNR penalty. Inset: OSNR penalty spread of the SOP string-length estimation method.

to follow the quartic dependence, we assume the penalty spread σ_1 of the pure first-order PMD string length to be caused by measurement errors. These errors are mainly due to the limited dynamic range of the camera and interpixel crosstalk due to power domination near the carrier frequency. Since the carrier signal is $\sim$10 dB higher than the sidebands, the signal was attenuated before the polarimeter to ensure that the carrier frequency did not saturate the camera readouts, thus sacrificing signal-to-noise in the SOP measurements of the sidelobes. The polarization crosstalk can be alleviated by increasing spectral resolution through optimization of the optical setup. VIPA has been reported to yield 3 dB spectral resolution of $\sim$600 MHz [10]. There is also $\sim$1 dB of uncertainty in the OSNR penalty measurement. The penalty spread σ is calculated as the standard deviation of the data points relative to the quartic fit, shown in Fig. 2(inset). Comparing the pure first-order PMD and all-order PMD measurements, we notice that the pure first-order data bounds the high order data from below, which agrees with previous observations [2]. To obtain the penalty spread σ' just due to the high-order PMD only [Fig. 2(inset)], we subtracted the spreading due to system error $\sigma' = (\sigma^2 - \sigma_1^2)^{1/2}$.

Next, we took a portable version of the spectral polarimeter to an AT&T central office for monitoring four OC-192 channels on a 250-km fiber route (mean DGD $= 15$ ps) carrying live data traffic between two major U.S. cities. These channels were experiencing performance instabilities where the pre-forward-error-correction (FEC) BER was fluctuating, and PMD was suspected to be one of the causes. The polarimeter was configured to allow only one channel to be measured at a time with a tunable filter preceding the polarimeter to eliminate multiple free-spectral ranges of the VIPA [6]. With a 2-D polarimeter [9], all channels within the C-band could be monitored in parallel. The spectral SOP of four channels was recorded once a minute for three days. It can be seen in polarization strings measured in a selected one hour duration shown in Fig. 3(a) that sometimes the strings only shift (polarization drift), while at other times they elongate indicating a change in the PMD-induced penalty. Fig. 3(b) showed that the string-lengths were less than 1 rad, or that the PMD on this fiber were causing less than 3 dB of penalty as indicated in Fig. 2. All four channels observed had the same string length statistics which were not correlated to the pre-FEC BER. Thus, it was concluded that the fluctuation in BER was not caused by PMD, and the system performance was not PMD-limited.

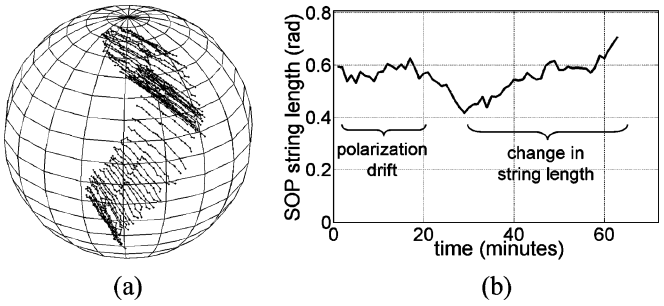

Fig. 3. (a) Sample SOP strings of one OC-192 channel recorded at one-minute intervals for over a one hour period, shown on Poincarè Sphere. (b) Variations of the sample SOP string-lengths over time.

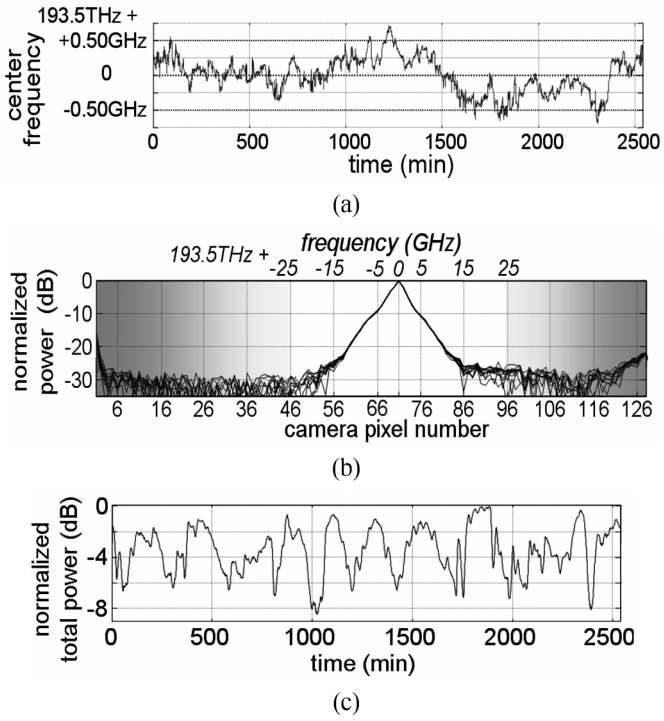

Fig. 4. (a) Center-frequency drift of an OC-192 channel observed using the spectral polarimeter. (b) Normalized power spectrum of the channel measured using the spectral polarimeter ($\sim$1 GHz/pix near pix#71); shaded regions indicate weaker diffraction orders of the VIPA. (c) Optical power fluctuations of the channel over a two-day period showing power fluctuations in the channel.

We also monitored center-frequency drift and total power fluctuation of each channel from the available spectral polarimeter data. Spatial location $\overline{\nu}$ of the center-frequency for each channel is estimated via the mean equation $\overline{\nu} = (\sum_{n=i}^{f} \nu_n P_n)/(\sum_{n=i}^{f} P_n)$, where P_n and ν_n are the power reading and wavelength, respectively, of pixel number n; i and f are, respectively, the starting and ending pixel numbers designated to that channel. Fig. 4(a) shows carrier-frequency tracking of an observed channel over a two-day period, and it can be seen that the carrier frequency drifted by $<$1.5 GHz, and was within the laser transmitter specification. The frequency variation did not appear to contribute to the observed BER fluctuations.

To obtain the power spectrum of a signal, two orthogonal polarization components measured by the polarimeter were summed. Fig. 4(b) shows a sample of normalized spectral profile of an OC192 channel measured ten times by the spectral polarimeter. Using a 12-bit InGaAs camera, the OSNR can be measured up to 33 dB. For each of the observed channels, powers were summed together from 41 pixels centered at the carrier-frequency pixel location [e.g., pixel #71 in Fig. 4(b)] to obtain the total power of the signal above the noise floor. The signal peaks outside the 41 pixel range [e.g., pixel #126 in Fig. 4(b)] are due to the weaker diffraction orders of the VIPA shown in the shaded region, which we ignored. Fig. 4(c) shows the monitored total power over two-day period. It can be seen that for this particular channel, the total power varied by as much as 8 dB. The power fluctuation was verified by an independent measurement, and the cause of the pre-FEC BER fluctuations was identified as a loss variation and traced to a faulty attenuator, which was eventually replaced.

III. Conclusion

We have demonstrated a nonintrusive PMD-induced penalty monitoring system using the SOP string length technique. We have shown in the laboratory and in the field that an SOP string length measurement can monitor system penalties due to PMD. While this has been a first-time demonstration of direct SOP string measurement in a system, further work is need to optimize the relationship between spectral SOP and high-order PMD penalty. The spectral polarimeter has also been shown to monitor other important system characteristics such as power and wavelength fluctuations, and we believe that it can contribute to the next-generation light-wave communication systems as a versatile performance monitoring device.

References

[1] C. J. Xie, L. Moller, R. M. Jopson, and A. H. Gnauck, "Efficiency of different feedback signals for polarization mode dispersion compensators," presented at the Proc. OFC Los Angeles, CA, 2004, Session WE4.

[2] M. Boroditsky, K. Cornick, C. Antonelli, M. Brodsky, S. D. Dods, N. J. Frigo, and P. Magill, "Comparison of system penalties from first and multiorder PMD," *IEEE Photon. Technol. Lett.*, vol. 17, no. 8, pp. 1650–1652, Aug. 2005.

[3] M. Boroditsky, M. Brodsky, N. J. Frigo, P. Magill, and J. Evankow, "Viewing polarization 'strings' on working channels: High-resolution heterodyne polarimetry," in *Proc. ECOC 2004*, Stockholm, Sweden, pp. 318–320.

[4] S. X. Wang and A. M. Weiner, "Fast wavelength-parallel polarimeter for broadband optical networks," *Opt. Lett.*, vol. 29, pp. 923–925, 2004.

[5] M. Shirasaki, "Large angular dispersion by a VIPA and its applications to a wavelength demultiplexer," *Opt. Lett.*, vol. 21, pp. 366–368, 1996.

[6] S. Xiao, A. M. Weiner, and C. Lin, "A dispersion law for virtually imaged phased-array spectral dispersers based on paraxial wave theory," *IEEE J. Quantum Electron.*, vol. 40, no. 4, pp. 420–426, Apr. 2004.

[7] I. Roudas, G. A. Piech, M. Mlejnek, D. Q. Chowdhury, and M. Vasilyev, "Coherent frequency-selective polarimeter for polarization mode dispersion monitoring," *J. Lightw. Technol.*, vol. 22, no. 4, pp. 953–967, Apr. 2004.

[8] L. Moller, P. Westbrook, S. Chandrasekhar, R. Dutta, and S. Wielandy, "SOP and PMD monitoring with WDM polarimeter," *Electron. Lett.*, vol. 38, pp. 583–585, 2002.

[9] S. X. Wang, S. Xiao, and A. M. Weiner, "Broadband, high spectral resolution 2-D wavelength-parallel polarimeter for dense WDM systems," *Opt. Express*, vol. 13, pp. 9374–9380, 2005.

[10] S. Xiao and A. M. Weiner, "Coherent Fourier transform electrical pulse shaping," *Opt. Express*, vol. 14, pp. 3073–3082, 2006.